Effects of NTC region on end-gas combustion modes under temperature stratification

Takahisa Nogawa, Hiroshi Terashima
Faculty of Engineering, Hokkaido University
N13 W8, Kita-ku, Sapporo, Hokkaido 060-8628, Japan

1 Introduction

Knocking is an abnormal combustion mode in spark-assisted ignition engines. Sometimes, knocking is accompanied by strong pressure wave generations such as detonations. Therefore, knocking has been a major obstacle in increasing the compression ratio and thermal efficiency of engines. To prevent knocking, several techniques have been successfully developed[1] such as retarding the ignition timing, using high-octane fuels, or introducing cooled exhaust gas recirculation. Temperature stratification is also a promising technique to prevent knocking[1]. The temperature in an engine cylinder is generally not uniform because of wall cooling, fuel vaporization, or swirl/tumble flows. Thus, several numerical studies have been performed recently for studying the effect of temperature stratification on end-gas combustion modes that focus on the occurrence of detonation[2,3]. These studies demonstrated that partial temperature gradients significantly affected the behavior of pressure wave generation associated with end-gas autoignition. In this study, we investigate the effects of spatial temperature stratification on the end-gas combustion modes during knocking. The unique features of this study are that the temperature stratification is distributed in the entire region of a reactor, and the end-gas combustion modes are realized under elevated pressure and temperature conditions. The effect of the negative temperature coefficient (NTC) region is also addressed by comparing the two fuels *n*-C_7H_{16} and *n*-C_4H_{10}.

2 Numerical method

We used the compressible Navier-Stokes equations with a thermally perfect gas equation of state, wherein we considered detailed transport models and chemical reaction mechanisms. A detailed description of the present method can be found in our previous studies[4,5].

Correspondence to: htera@eng.hokudai.ac.jp

3 Numerical model and conditions

Knocking combustion was modeled using a 1-D reactor, as shown in Fig. 1. The length of the reactor was 4 cm (considering the scale of the actual engine). The symmetric condition was used for the left boundary and the adiabatic wall condition was assumed for the right boundary. The initial pressure was 5 atm. We considered two premixed gases: stoichiometric n-C_7H_{16}/air and n-C_4H_{10}/air mixtures. The reaction mechanisms were generated by KUCRS[6]; n-C_7H_{16} consists of 373 species and 1071 reactions, and n-C_4H_{10} consists of 113 species and 426 reactions. Figure 2 shows the ignition delay times of the two premixed gases at 5 atm numerically obtained under adiabatic conditions; this indicates that the NTC region distinctly appears in the n-C_7H_{16} case. A flat hot-kernel of 1400 K with a length of 0.1 cm was initially inserted into the left side to initiate the flame front propagation. For considering temperature stratification, we assumed a linear spatial gradient and defined two parameters: the temperature at the center of the reactor (T_c) and the spatial gradient ($\mathrm{d}T/\mathrm{d}x$). The center temperature T_c parametrically changed from 600 K to 900 K, and $\mathrm{d}T/\mathrm{d}x$ was set to the values –10, –5, –1, –0.5, and –0.1 K/cm. For reference, we have shown a case with 900 K and –10 K/cm in Fig. 3.

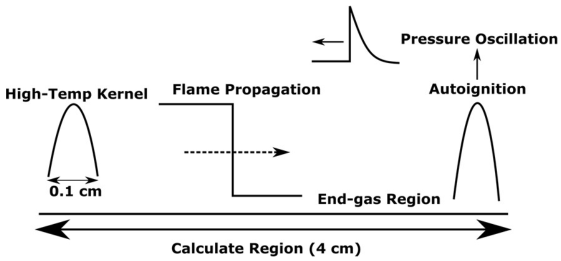

Figure 1. Schematic of the one-dimensional constant volume reactor

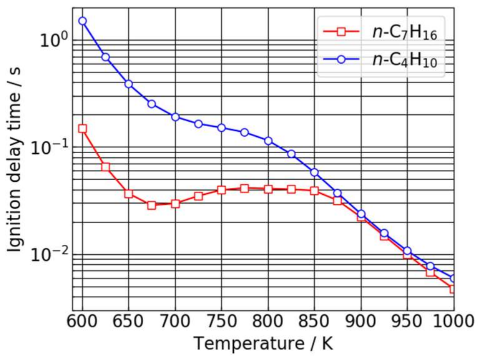

Figure 2. Comparison of the ignition delay time under constant volume and adiabatic conditions

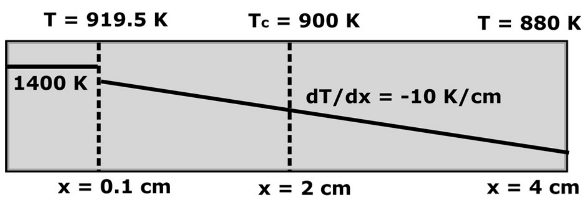

Figure 3. Schematic of a temperature gradient case

4 Results and discussion

4.1 Knocking Intensity

The knocking intensity (KI) is defined as follows:

$$\mathrm{KI} = P_{\mathrm{max}}/P_{\mathrm{e}} \tag{1}$$

Here P_{max} is the first peak in the maximum pressure history, and P_{e} is the equilibrium pressure in the reactor. Therefore, the KI is a metric that represents how a pressure wave is developed in the end-gas region.

4.2 Result of n-C_4H_{10}

The left-hand side of Fig. 4 shows the KI of n-C_4H_{10}/air mixture against the temperature gradients; the results are shown for four reactor center temperatures. It is shown that large temperature gradients, such as –10 K/cm, have small KIs for all the temperature conditions. However, larger KIs can be observed with small temperature gradients, such as with –1 K/cm and –0.5 K/cm, only in high-temperature conditions.

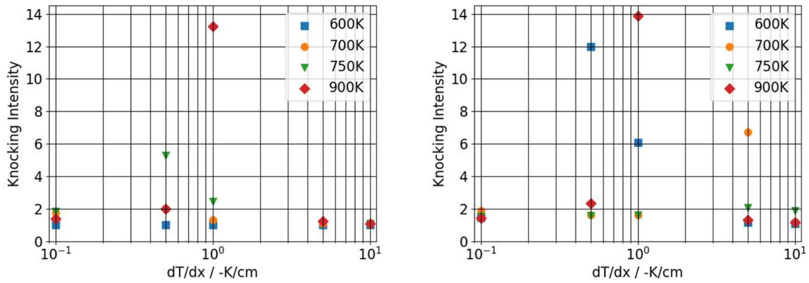

Figure 4. Variation in KIs with the temperature gradients for n-C_4H_{10} (left) and n-C_7H_{16} (right)

To identify the KI trend, we discuss the detailed mechanisms for end-gas autoignition and pressure wave development using the results obtained at 900 K. Figure 5(a) shows the temporal sequence of pressure and temperature profiles in the end-gas region in the case of no temperature gradient. Autoignition occurs almost simultaneously in the whole end-gas region; therefore, a pressure wave is not strongly developed. However, the profile with a large gradient of –10 K/cm in Fig. 5(b) presents a completely different end-gas combustion mode. End-gas autoignition successively occurs from the flame front, which propagates at an average speed of 60 m/s; this speed is higher than that for the deflagration mode, but much less than the speed of sound. Therefore, pressure variations are substantially reduced, which results in smaller KIs. Figure 5(c) shows the result with a smaller temperature gradient of –1 K/cm. End-gas autoignition begins to occur near the flame front similar to the –10 K/cm case. However, the pressure wave generated becomes stronger through propagation in the end-gas region, which is caused by a coupling between the pressure wave and the successive end-gas autoignition front. It should be noted that there is a difference in the time intervals of each profile between the results with –10 K/cm and –1 K/cm.

According to the studies by Zeldovich and Bradley[7,8], the end-gas combustion mode is primarily governed by the spatial gradient of the ignition delay times (and the speed of sound). Therefore, to address the generation of different combustion modes, we investigated the spatial gradient distribution of the ignition delay times. Figure 6 makes a comparison between the ignition delay times for the gradients of –10 K/cm and –1 K/cm at 900 K. It can be seen that smaller temperature gradients generate smaller gradients of ignition delay times, and the variation is monotonic in the whole region. The spatial gradient of the ignition delay times affects the propagation speed of the successive autoignition front; therefore, different combustion modes are realized in the end-gas region.

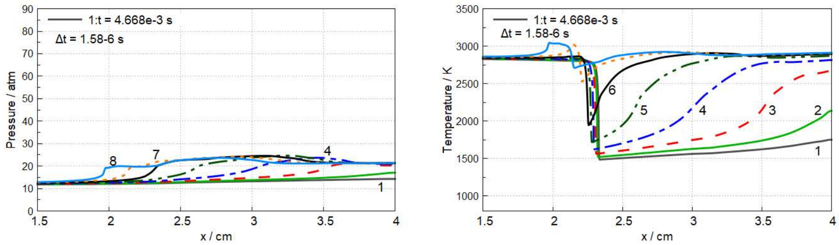

(a) No gradient

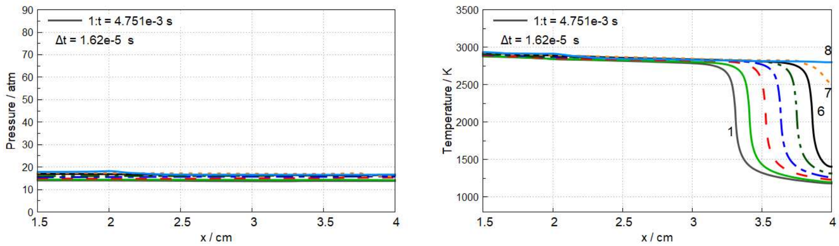

(b) $\mathrm{d}T/\mathrm{d}x = -10$ K/cm

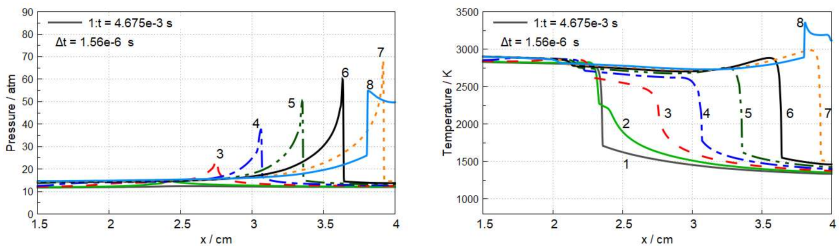

(c) $\mathrm{d}T/\mathrm{d}x = -1$ K/cm

Figure 5. Sequential profiles of pressure and temperature distributions

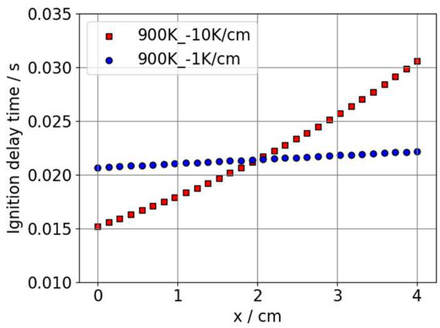

Figure 6. Spatial distribution of ignition delay times for temperature gradients of –10 K/cm and –1 K/cm

4.3 Result of n-C_7H_{16}

The right-hand side in Fig.4 shows the KI for the case of the n-C_7H_{16}/air mixture. Similar to the result of n-C_4H_{10}, the KI has peaks with relatively small temperature gradients, whereas large temperature gradients can maintain smaller knocking intensities. One unique feature of n-C_7H_{16} is that the KI becomes large even for large temperature gradients; another peak is generated at –5 K/cm for 700 K.

Figures 7(a) and 7(b) show the pressure and temperature profiles of n-C_4H_{10} and n-C_7H_{16}, respectively, at 700 K. The results for n-C_4H_{10} show successive end-gas autoignition behavior (similar to the results obtained for –10 K/cm at 900 K in Fig. 5(b)). However, the results for n-C_7H_{16} show a developing detonation mode with the generation of a large pressure peak. Thus, the appearance of such different combustion modes even under the same temperature gradient may indicate the effect of the NTC region on the end-gas autoignition mode. Figure 8 shows a comparison of the spatial distribution of n-C_4H_{10} and n-C_7H_{16} for the ignition delay times at 700 K and –5 K/cm. The result using n-C_4H_{10} shows a trend similar to that in 900 K and –10 K/cm (see Fig. 6). However, the result using n-C_7H_{16} shows a unique non-monotonic behavior because of the presence of the NTC region in the ignition delay times. Therefore, the spatial gradient of the ignition delay times is significantly different between n-C_4H_{10} and n-C_7H_{16} even under the same center temperature. The developing detonation mode in the case of n-C_7H_{16} is induced by the appearance of such a small gradient distribution of the ignition delay times in the end-gas region.

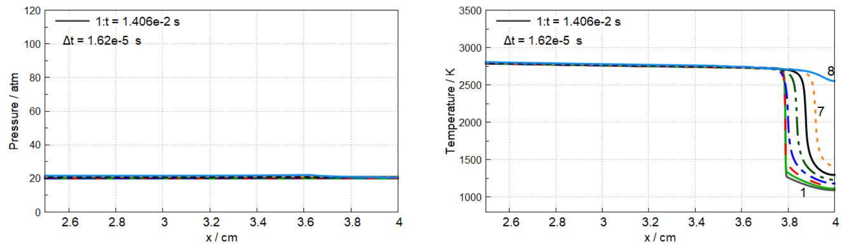

(a) T_c = 700 K, $\mathrm{d}T/\mathrm{d}x$ = –5 K/cm for n-C_4H_{10}

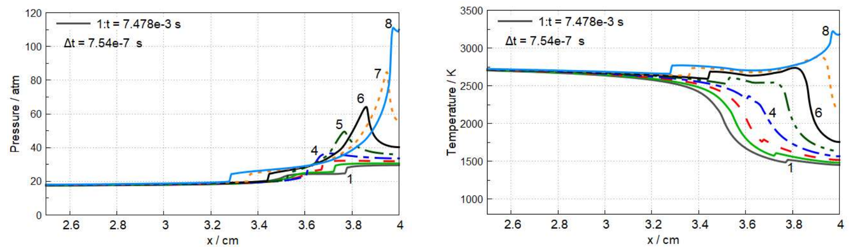

(b) T_c = 700 K, $\mathrm{d}T/\mathrm{d}x$ = –5 K/cm for n-C_7H_{16}

Figure 7. Sequential profiles of pressure and temperature distributions

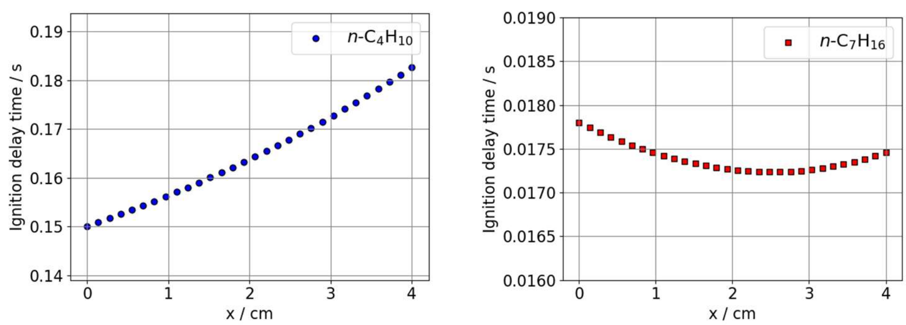

Figure 8. Distribution of ignition delay times for n-C_4H_{10} (left) and n-C_7H_{16} (right)

5 Conclusions

We numerically investigated the effects of temperature stratification on the combustion modes associated with end-gas autoignition. The two fuels n-C_4H_{10} and n-C_7H_{16} were used for identifying the effect of the NTC region on the end-gas combustion modes. The result demonstrates that large temperature gradients can suppress severe pressure peaks through the appearance of successive end-gas autoignition modes. In contrast, smaller temperature gradients produce high-pressure peaks with the generation of a developing detonation mode. The comparison between n-C_4H_{10} and n-C_7H_{16} shows a significant impact of the NTC region on the spatial distribution of ignition delay times and thereby on the end-gas combustion modes. The NTC region may increase the possibility of a developing detonation mode. In the final presentation, higher-pressure cases will be considered and a classification of the combustion modes with the spatial gradient of the ignition delay time and excitation time will be conducted.

References

[1] Z. Wang, H. Liu, R.D. Reitz, (2017). Knocking combustion in spark-ignition engines. Prog. Energy Combust. Sci. 61 :78.

[2] A. Sow, B.J. Lee, F.E. Hernández Pérez, H.G. Im, (2018). Detonation onset in a thermally stratified constant volume reactor. Proc. Combust. Inst. 37 :3529.

[3] P. Dai, Z. Chen, S. Chen, Y. Ju, (2015). Numerical experiments on reaction front propagation in n-heptane/air mixture with temperature gradient. Proc. Combust. Inst. 35 :3045.

[4] H. Terashima, M. Koshi, (2015). Mechanisms of strong pressure wave generation in end-gas autoignition during knocking combustion. Combust. Flame. 162 :1944.

[5] H. Terashima, A. Matsugi, M. Koshi, (2017). Origin and reactivity of hot-spots in end-gas autoignition with effects of negative temperature coefficients: Relevance to pressure wave developments. Combust. Flame. 184 :324.

[6] A. Miyoshi, (2011). KUCRS – Knowledge-basing Utilities for Complex Reaction Systems –. http://akrmys.com/KUCRS/index.htm.ja.

[7] Y.B. Zeldovich, (1980). Regime classification of an exothermic reaction with nonuniform initial conditions. Combust. Flame. 39 :211.

[8] X.J. Gu, D.R. Emerson, D. Bradley, (2003). Modes of reaction front propagation from hot spots. Combust. Flame. 133 :63.